Acoustical Imaging and Mechanical Properties of Soft Rock and Marine Sediments
(Quarterly Technical Progress Report #15302R06)

Reporting Period: 04/01/02 - 06/31/02

Thurman E. Scott, Jr., Ph.D.
Younane Abousleiman, Ph.D.
Musharraf Zaman, Ph.D., P.E.

Report Issued: November 18, 2002

DOE Award Number: DE-FC26-01BC15302

PoroMechanics Institute
The University of Oklahoma
Sarkeys Energy Center, Room P-119
100 East Boyd Street
Norman, Oklahoma 73019-1014

DISCLAIMER

ABSTRACT

During the sixth quarter of this research project the research team developed a method and the experimental procedures for acquiring the data needed for ultrasonic tomography of rock core samples under triaxial stress conditions as outlined in Task 10. Traditional triaxial compression experiments, where compressional and shear wave velocities are measured, provide little or no information about the internal spatial distribution of mechanical damage within the sample. The velocities measured between platen-to-platen or sensor-to-sensor reflects an averaging of all the velocities occurring along that particular raypath across the boundaries of the rock. The research team is attempting to develop and refine a laboratory equilvalent of seismic tomography for use on rock samples deformed under triaxial stress conditions. Seismic tomography, utilized for example in crosswell tomography, allows an imaging of the velocities within a discrete zone within the rock. Ultrasonic or acoustic tomography is essentially the extension of that field technology applied to rock samples deforming in the laboratory at high pressures.

This report outlines the technical steps and procedures for developing this technology for use on weak, soft chalk samples. Laboratory tests indicate that the chalk samples exhibit major changes in compressional and shear wave velocities during compaction. Since chalk is the rock type responsible for the severe subsidence and compaction in the North Sea it was selected for the first efforts at tomographic imaging of soft rocks. Field evidence from the North Sea suggests that compaction, which has resulted in over 30 feet of subsidence to date, is heterogeneously distributed within the reservoir. The research team will attempt to image this very process in chalk samples. The initial tomographic studies (Scott et al., 1994a,b; 1998) were accomplished on well cemented, competent rocks such as Berea sandstone. The extension of the technology to weaker samples is more difficult but potentially much more rewarding. The chalk, since it is a weak material, also attenuates wave propagation more than other rock types. Three different types of sensors were considered (and tested) for the tomographic imaging project: 600 KHz PZT, 1 MHz PZT, and PVDF film sensors. 600 KHz PZT crystals were selected because they generated a sufficiently high amplitude pulse to propagate across the damaged chalk. A number of different configurations were considered for placement of the acoustic arrays. It was decided after preliminary testing that the most optimum arrangement of the acoustic sensors was to place three arrays of sensors, with each array containing twenty sensors, around the sample. There would be two horizontal arrays to tomographically image two circular cross-sectional planes through the rock core sample. A third array would be vertically oriented to provide a vertical cross-sectional view of the sample. A total of 260 acoustic raypaths would be shot and acquired in the horizontal acoustic array to create each horizontal tomographic image. The sensors can be used as both acoustic sources or as acoustic each of the 10 pulsers to the 10 receivers.

TABLE OF CONTENTS

ABSTRACT 3
LIST OF GRAPHICAL MATERIALS 5
INTRODUCTION 6
EXECUTIVE SUMMARY 7
EXPERIMENTAL 8
REFERENCES 11
LIST OF ACRONYMS AND ABBREVIATIONS 12

LIST OF GRAPHICAL MATERIALS FOR THE PROJECT

TABLE 1 – Project time line with the first, second, third, fourth, fifth, and sixth quarter targets highlighted 13

FIGURE 1a – A schematic of the locations of the acoustic pulse transmission sensors on the rock core sample 14

FIGURE 1b – A schematic of the equipment for the ultrasonic tomography experiment 15

FIGURE 2 – Locations of the acoustic pulse transmission sensors on the sample 16

FIGURE 3 – A 3-dimensional view of the acoustic tomographic pulse transmission array 17

FIGURE 4 – A top view of the acosutic raypaths in a horizontal plane 18

FIGURE 5 – 3 dimensional locations of the horizontal tomographic imaging planes 19

FIGURE 6 – A side view of acoustic raypaths in the X-Y plane 20

FIGURE 7 – A 3-dimensional view of the acoustic raypaths in the vertical imaging plane. . . . 21

FIGURE 8 – A 3-dimensional view of all the acoustic raypaths in the rock sample. There are a total of 620 acoustic raypaths in the projection. 22

INTRODUCTION

Acoustic tomography on laboratory scale rock samples represents a technique for determining the variations in velocity heterogeneities in samples undergoing deformation.
The method is based on measuring the acoustic (or seismic) velocities along a large number of raypaths and then these velocities are used to reconstruct a 2-dimensional internal image of a rock section. Stacking a series of 2-D images can provide a three-dimensional internal image of a volume of rock. The technique was first used in the mid 1970's principally in cross-well tomography and has been used to map rock lithologies, track CO_2 floods, fire floods, and waterfloods during petroleum enhanced recovery operations (Bregman et al. 1989; Justice et al., 1989; Johnston 1997).

Acoustic (ultrasonic) tomography has also been used in the laboratory to image:

1) dilatancy created during triaxial compressive failure (Yanigadani et al. (1987). In this case the development of microcracking resulted in slower acoustic velocities.

2) hydraulic fracturing in granite samples (Falls et al., 1992). In this study a mode I fracture was detected from the lower wave velocities in the vicinity of the crack.

3) elastic stress distributions (Scott et al., 1994a,b), during compressive indentation testing. In these tests the elastic closure of microcracks in highly stressed regions of a rock exhibited higher velocities.

4) compactive failure during indentation experiments (Scott et al., 1998). In that study the compressional wave velocities decreased due to the breakage of cements between the grains during compaction.

The advances in ultrasonic tomographic imaging will be in its use under triaxial (e.g., high confining pressure) conditions as this is the stress condition which best approximates those which occur in the subsurface. Only the study of Scott et al., (1998) was conducted under such conditions. To date no other experiments utilizing tomographic imaging have been conducted under triaxial stress conditions. The major difficulty, and the reason so few experiments are conducted to tomographically image rocks under pressure, is due to the problem in sealing a large number of electrical leads (for the acoustic sensors) through the pressure jacket of the rock sample.

It should be noted that there is a major difference between the field uses of seismic tomography and the laboratory uses of ultrasonic tomography. Seismic tomography in the field is primarily utilized to image 1) rock lithologies, or 2) changes in pore fluid properties (e.g., oil/water displacement during CO_2 flooding). While acoustic (ultrasonic) tomography in the laboratory is generally undertaken to image changes in rock properties (e.g., elastic deformation) or rock damage (e.g., fracturing). In the current research program, the research team will image compactive soft rocks to determine the heterogeneity of damage.

EXECUTIVE SUMMARY

During this phase of the project the research team began to: 1) analyze some of the acoustic velocity data, and 2) continued an investigation of the deformation of sand at high pressures to simulate the shallow water flow problem. One of the goals of the study is to create a series of `deformation-velocity' maps for each of the various rock types in the project. The deformation-velocity maps involve correlating rock damage mechanisms, e.g., compaction, dilation etc., to their specific acoustic velocity signatures. By making such a host of such correlations the research team will be able to predictively determine the type of damage and its specific acoustic compressional and shear wave signature when the rock undergoes specific changes in effective stress (for example during drawdown production from an oil and gas reservoir). In this report the research team presents some of the initial compressional and shear wave velocity data on Danian chalk. This high porosity, weakly cemented chalk, is thought to be an excellent analog to the Ekofisk chalk of the North Sea which has created severe compaction and subsidence problems for the petroleum industry. During a hydrostatic compression experiment the Danian chalk exhibited remarkable changes as the pressure increased. Some of the preliminary data indicates that the acoustic velocities in the chalk decreased by as much as 200 m/s during the initial onset of damaging compaction. In addition, the research team continued to analyze results from the sand deformation experiments conducted at confining pressures. These sand experiments are designed to reproduce the problem of shallow water flows which have been so problematic for the petroleum industry conducting deepwater drilling operation in the U.S. Gulf Coast. Preliminary experiments indicate that liquefaction, which is thought to be analogous to the shallow water flow problem, can occur at high confining pressures in sand. Some of the experiments were conducted on Oil Creek sand with different amounts of fines added to the sand. The preliminary results suggest that sands with 10% added fines can undergo liquefaction at lower stress conditions than sand samples which do not have fines added.

EXPERIMENTAL METHOD (Tomography)

Several methods were considered for the geometrical arrangement of acoustic sensors and tomographic imaging planes within the triaxial core samples. This progress report basically outlines the configuration for the various testing procedures. It should be noted that the complexity of wave propagation and data acquisition from these samples does present problems which are continually being addressed. Initially, the research team proposed to tomographically image the rock along three horizontal planes and one vertical plane to locate and discern the degree of uniformity of the deformational mechanisms within the rock (particularly in regard to compaction). Preliminary pulse transmission work indicated that there would be severe problems with imaging near the boundaries of the core sample. At this time the research team plans to utilize cylindrical samples of chalk for testing with a diameter of 10 cm and length of 20 cm. Acoustic tomographic imaging will be accomplished (initially) on three planes oriented within the samples (Figure 1a). One image will be made vertically and two will be made horizontally. Approximately 60 acoustic sensors will be used in three arrays around the sample. (Note an array is defined as the 20 sets of sensors on each plane). Figure 1a shows a schematic of the locations of the sensors on a cylindrical rock sample.

The equipment utilized in making acoustic tomography measurements is shown in Figure 1b. It consists of a 1) Tektronix TDS 420 digital storage oscilloscope, 2) a HP switchbox, and 3) an array of acoustic sensors mounted on the rock sample (see Figure 1b). Any acoustic sensor can be used as a source or receiver in the current configuration. The acoustic sensors are made in-house (see first quarterly progress report for details). Two methods were considered for acquisition of the tomographic images. This method involves firing one pulse and receiving one wave. Scott et al. (1994a,b; 1998). The method has the technical disadvantages in that 1) it is inefficient since it requires 620 pulses (one from each sensor-receiver pair), and 2) it requires several minutes to complete the waveform acquisition process. It should be noted that the technical acquisition of tomogram is every bit analog to obtaining a photograph from a camera where the shutter lens is held open for a long period of time. The longer the lens remains opens (or in the case of topography the longer it takes to obtain all the raypaths) the more potential that the subject to be imaged may undergo changes. In the case of a rock sample undergoing damage at high pressures, the process is continually evolving so it would be advantageous to complete the acquisition in the shortest time possible. Ideally, the best way to shoot the tomogram would be to use a minimum of 60 pulses and record the waves on each of the other 20 sensors in a given array. This is how field seismic measurements are accomplished. The big problem with using this same method on a core sample is that a geometrical array of piezoelectric receiver crystals have characteristics that are strongly influenced by their size and their geometrical position relative to the acoustic source. Given this problem it is advantageous to use a DSO to acquire the acoustic waves since scaling of the received wave can be easily changed to accommodate changes in the amplitude of the waveforms. Stated succinctly, we are trading for the enhanced clarity of the acquired waveforms at the expense of speed in acquisition of those waveforms.

One of the problems facing the research team is how to accomplish command and control of the data acquisition process for the tomographic waveform data. The current research process is much more difficult than the earlier approach of Scott et al., 1994a,b; 1998). In the current case, multiple arrays are utilized (three instead of one in the earlier studies) and the arrays have a different geometry (rectangular versus circular). In order to simplify the process (for this particular experiment only) the raypaths are visually plotted on an IBM-PC (Figures 2 to 8). Figure 2 provides a top and two sides views of the 60 sensors arranged around the core sample. Figure 3 provides a 3-dimensional view of the location of the acoustic sensors. In the horizontal plane (Figure 4) a total of 260 raypaths are acquired in the proposed setup. A single pulsed wave is received by 13 of the surrounding receiving sensors. The six closest sensors adjacent to the pulsed sensor (three on either side) are rejected for acquisition in the array as the first arrival is difficult to detect at such low acceptance angles of the sensor. Each of the 20 sensors is pulsed with the 13 raypaths of the fan beam until the symmetry observed in Figure 4 is completed. On a 10cm diameter core sample this coverage is sufficient to provide a 1.0cm pixel resolution in the imaging process. Figure 5 shows the 3-dimensional orientation of a stack of the two horizontal slices within the cylindrical sample. Figure 6 is a side view of the 100 acoustic raypaths to be acquired in the vertical slice in the core sample. There are twenty sensors (ten on each side of the sample). In this array each of the ten sensors on one side represents the pulses and the ten on the opposite side represent the receivers. Two aspects of the raypath patterns in this vertical plane are very different from the horizontal planes. First, the raypath fan beams are not symmetrical but vary from pulser to pulser. Second, the coverage at the ends of the rectangular cross section is extremely limited (Figure 5 and 6). This is due to the fact that the steel end platens preclude the placement of acoustic sensors in this region of the sample. The poor coverage is typical of and directly analogous to the problems encountered in crosswell tomography when sensor coverage is poor. Figure 7 is a 3-dimensional view of the vertical array of the acoustic raypaths in the rock sample. Figure 8 shows a 3-dimensional diagram of all the computer raypaths to be acquired in the experiment. Again, there will be a total of be 620 acoustic compressional waves acquired with 260 on each of the two horizontal planes and 100 on the vertical plane.

Imaging on the horizontal planes also presented a new set of challenges. In previous research (Scott et al. 1994a,b; 1998) 1 MHz sensors were utilized on denser and stronger samples of Berea sandstone and Cordoba Cream limestone. Chalks present problems due to the high attenuation of the acoustic waves propagating through the weaker material. 1 MHz sensors were abandoned as they were deemed to have insufficient pulse amplitude to propagate an identifiable wave in a highly damaged chalk sample at the boundaries of the acceptance angle of these sensors. 600 KHz and PVDF sensors were both considered. PVDF were tested and abandoned. They made great receivers but had poor pulse characteristics. 600 KHz sensors are much more energetic than 1 MHz sensors. The problem is that the footprint of a 600 KHz sensor nearly double that of a 1 MHz sensor. In our acoustic research we attempted to keep the width-to-diameter ratio at one or greater than one. W/D ratio be maintained at 1. The primary reason for this is that sensor with a W/D less than one seem to develop extreme poor resonant properties. The 600 KHz sensors have a width of 0.6 cm and this is a considerable footprint in relation to the size of the sample. (Note also that 600 KHz sensors are nearly twice as thick as 1 MHz). Ideally, sensors should be point sources but from a practical standpoint small sensors cannot create enough pulsed energy to be detectable. The problem of the sensors not being actually point sources becomes a major problem to sensors on the margins of the fan beam. A fan beam is the collection of raypaths pulsed from a single source sensor (in the case of this study it is 110^{o}). Great care must be utilized for identifying the first arrivals of sensors on the margins of the fan beam due to the fact that the first arrival might be from the extreme edge of the pulsed sensor to the extreme edge of the received sensor and not from the center-to-center of the sensors. A preliminary test to evaluate this problem indicates that the research team will be able to adequately detect the proper wave velocity for even these raypaths.

The research team also evaluated the potential for problems that could be created by wrongly identifiying surface wave arrivals which mask body wave arrivals. Generally, surface waves are much slower than internal body waves. However, the large footprint (0.6cm) of each of the 600 KHz piezoelectric elements is made even larger by gluing, grounding, and shielding the sensors on the rock sample. Collectively, the twenty sensors can create a high velocity pathway around the circumference of the rock. In a high velocity rock this is not a problem (e.g., the tests of Scott et al., 1994a,b; 1998). In a low velocity rock (e.g., chalk) it could potentially be a large problem. The surface wave, traveling around the circumference from sensor to sensor and along its grounding wires (if improperly connected), can arrive at opposing receivers faster than the body wave propagating directly through the diameter of the rock sample. Preliminary work indicates that this will not be a problem for the chalk experiment. The research team decided the best way to minimize such an effect was by mounting the sensors with epoxies and glues having a low Young's moduli and by attempting to keep the connecting wires directly off the surface of the rock core sample.

There are two additional notes that should be made in regards to acquisition of the tomograms. First, the principal of reciprocity states the velocity measured from a pulsed wave from one pair of sensors should be the same no matter which is used as the source. If one assumes this principal is true and that during a post-test analysis of acoustic wave data it was discovered that the waves were not the same then it can impact whether to accept the data as valid. For example, if a pulse were fired and acquired from sensor 1 to sensor 8 and later the wave acquired from 8 back to 1, and these exhibited significant velocity differences then something may be wrong. The most obvious occurrence would be that the damage process within the rock is evolving faster than the tomographic imaging acquisition can be completed (i.e., analogous to the camera shutter problem again).

Preliminary tests indicate that it would be best to pulse each raypath two times to insure adequate acquisition of the waves. The arrival time of each wave will be identified manually to insure accuracy. The tomograms will be generated in two forms. Absolute velocity images which records the exact velocities and difference imaging which involves subtracting successive velocity images from the initial image to track changes as deformation occurs. These have been successfully used by Scott 1994a and Scott 1994b. Of these, the difference imaging technique seems to have more visual impact for highlighting regions of the rock sample where more velocity changes are occurring. In addition, these types of tomograms can highlight changes that are difficult to detect in absolute tomograms, particularly in cases where the changes are tensile relative to compression.

References

Bregman, N.D., Hurley, P.A., and West, G.F.: ``Seismic Tomography at a Fire Flood Site,'' Geophysics (1989), 54, 1082-1090.

Falls, S.D., Young, R.P., Carlson, S.R., and Chow, T., 1992, Ultrasonic tomography and acoustic emission in hydraulically fractured Lac du Bonnet grey granite, J. Geophys. Res. 97, B5, pp. 6867-6884.

Justice, J.H., Vassiliou, A.A., Logel, J.D., Hansen, P.A., Hall, B.R., Hutt, P.R., and Solanki, J.J.: ``Acoustic Tomography for Monitoring Enhanced Oil Recovery,'' Geophysics, The Leading Edge of Exploration (1989) 8, no. 2, 12-19.

Johnston, D.H.: ``A Tutorial on Time-Lapse Seismic Reservoir Monitoring,'' OTC 8289 (1997).

Scott, T.E., Ma, Q., Reechoes, Z., and Roegiers, J.- C., 1994a, Dynamic stress mapping utilizing ultrasonic tomography, The Proceedings of the 1st North American Rock Mechanics Symposium, Nelson and Laubach (eds), Balkema, Rotterdam.

Scott, T.E., Ma, Q., Roegiers, J.-C., and Reches, Z., 1994b, Acoustic tomographic difference imaging of dynamic stress fields, presented in EUROCK 94, Aug. 29-31, Delft, The Netherlands, Rock Mechanics in Petroleum Engineering, Balkema, Rotterdam.

Scott, T.E., Zaman, M.M., and Roegiers, J.-C., (1998) Acoustic velocity signatures associated with rock-deformation processes, Journal Petroleum Technology, (SPE39403), Vol. 50, No. 6, pp. 70-74.

Yanagidani, T., Yamada, H., and Terada, M., 1987, The observation of faulting process in rock by computer tomography, (in Japanese with English abstract), J. Soc. of Civil Engineering, 382, pp. 73-82.

LIST OF ACRONYMS AND ABBREVIATIONS

PVDF = Polyvinylindine Fluoride (a piezoelectric polymer)

DSO = Digital Storage Oscilloscope

Project month	1	2	3	4	5	6	7	8	9	10	11	12	13	14	15	16	17	18	19	20	21	22	23	24
Task 1 Obtain Rock Samples	X	X																						
Task 2 Construct New Acoustic Platens	X	X																						
Task 3 Calibrate Equipment	X	X																						
Task 4 Prepare Sandstone & Chalk Samples		X	X	X																				
Task 5 Construct Lateral Acoustic Sensors		X	X	X																				
Task 6 Reconnaissance Test Chalk & Sandstones				X	X	X																		
Task 7 AE Hypocentral Location & Full Dynamic Tensor							X	X	X	X	X													
Task 8 Correlate Static & Dynamic Parameters											X	X												
Task 9 Test Sand Pack Samples													X	X	X									
Task 10 Ultrasonic Tomography on Sandstone & Chalks																X	X	X	X	X				
Task 11 Make Deformation Velocity Maps																					X	X		
Task 12 Final Report																							X	X

Table 1: Project time line with sixth quarter targets highlighted

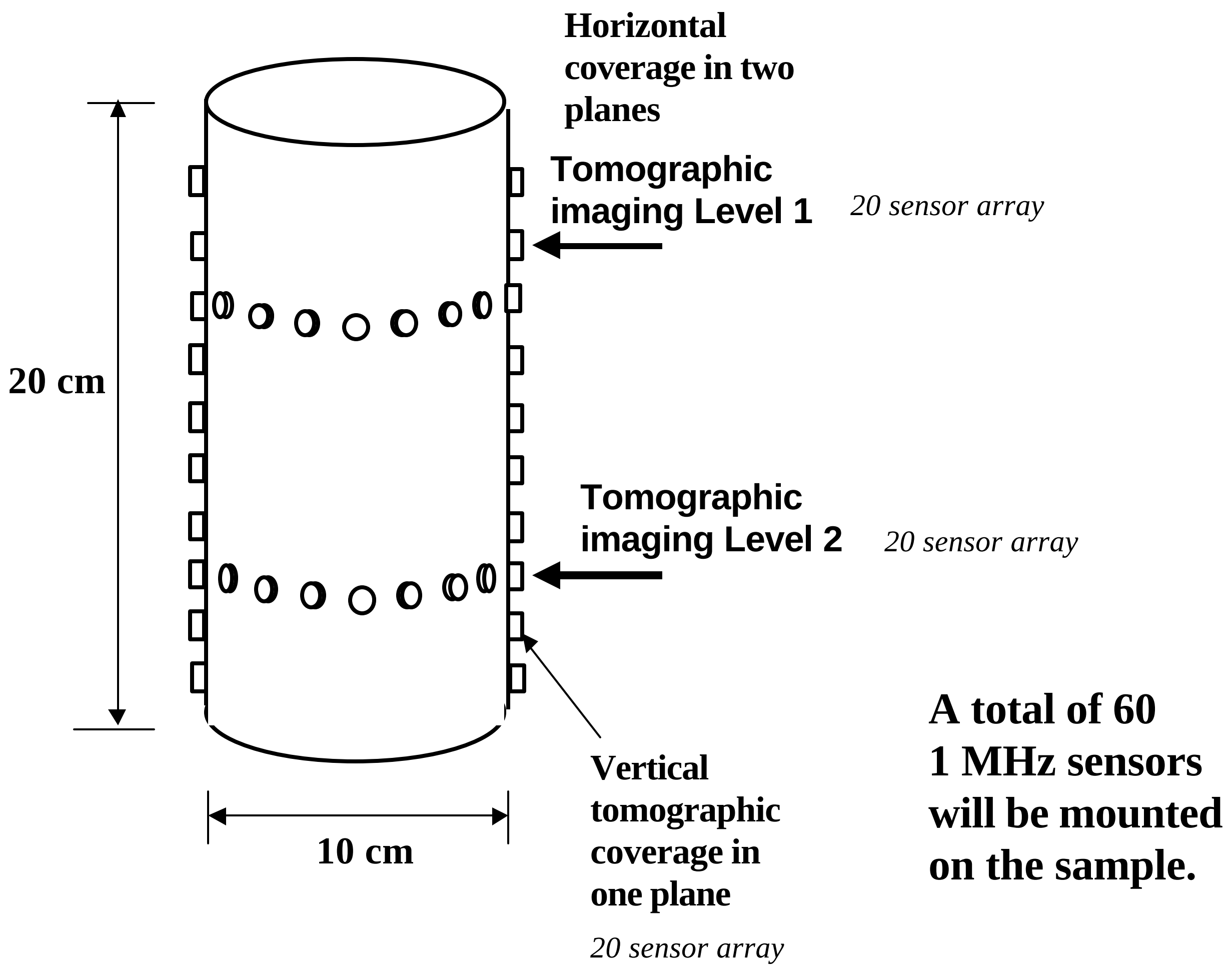

Figure 1a. A schematic of the locations of the acoustic pulse transmission sensors on the rock core sample.

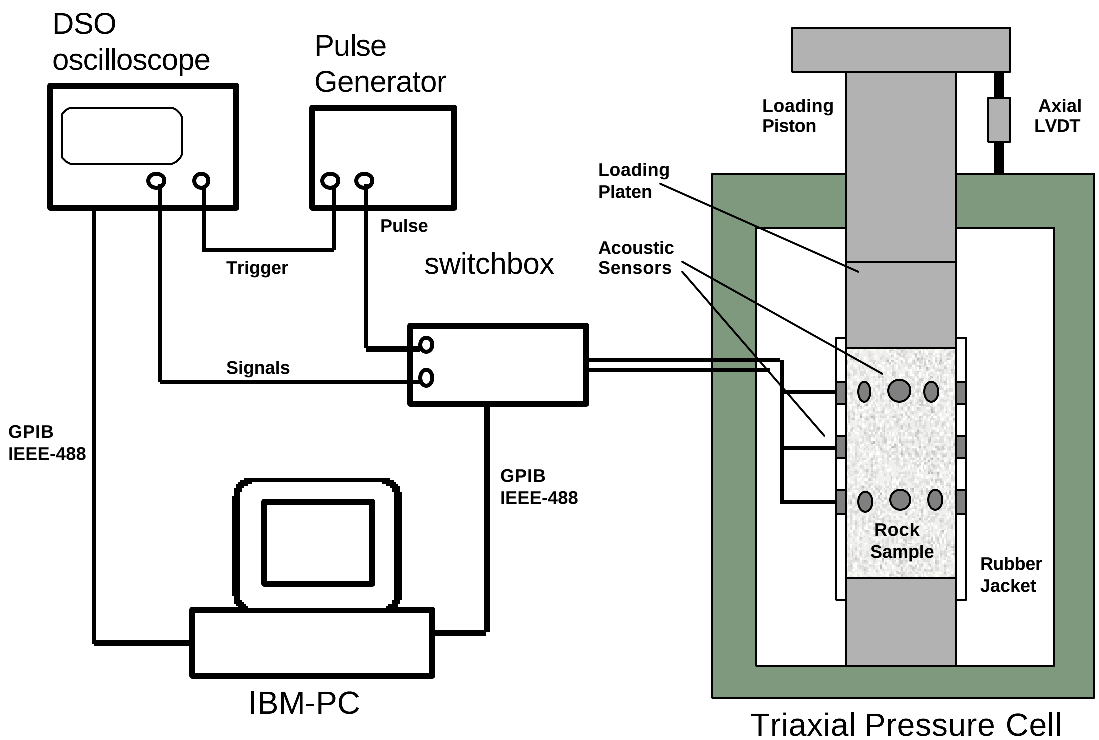

Figure 1b. A schematic of the equipment for the ultrasonic velocity experiment.

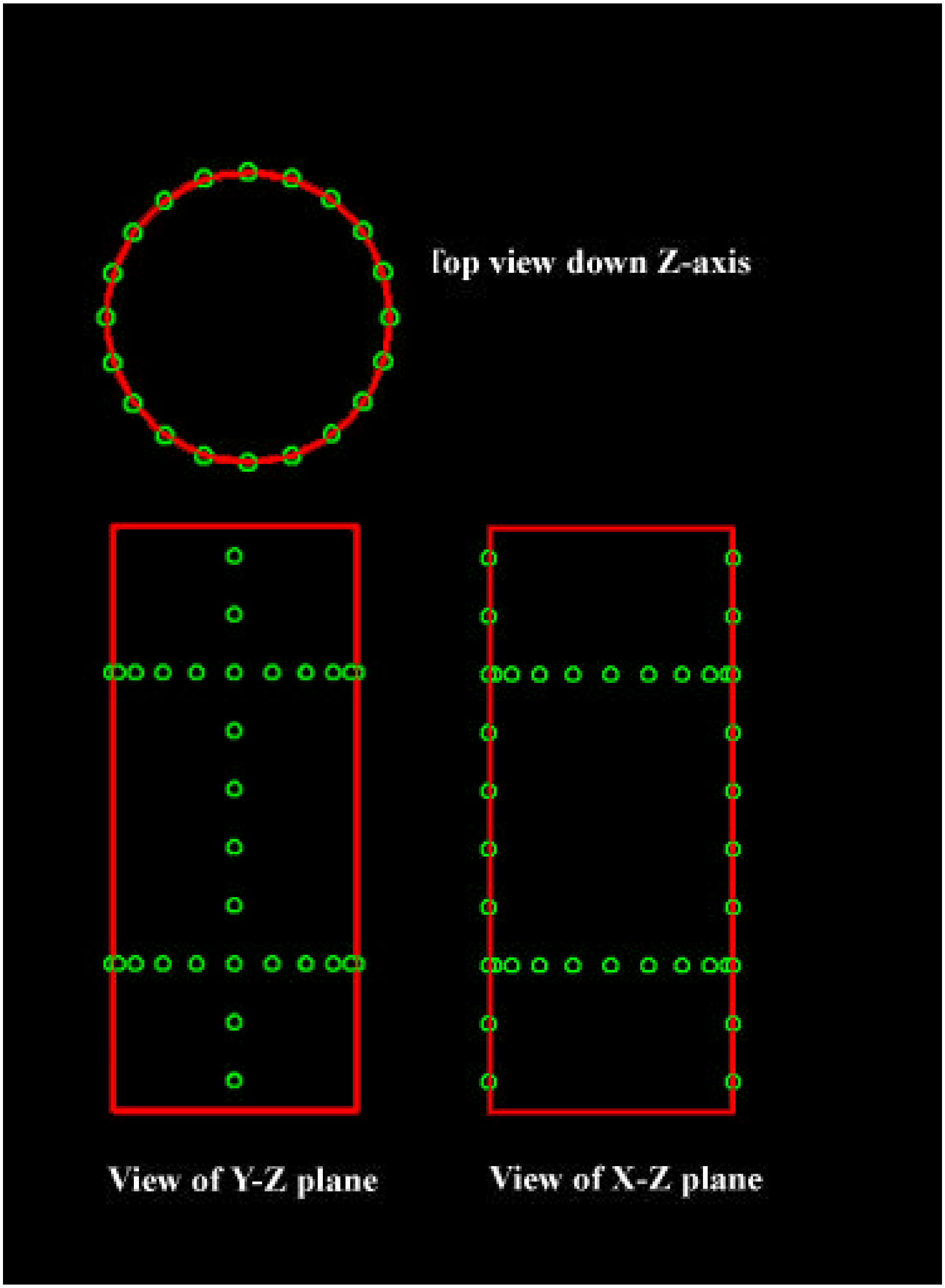

Figure 2. Locations of the acoustic pulse transmission sensors on the sample.

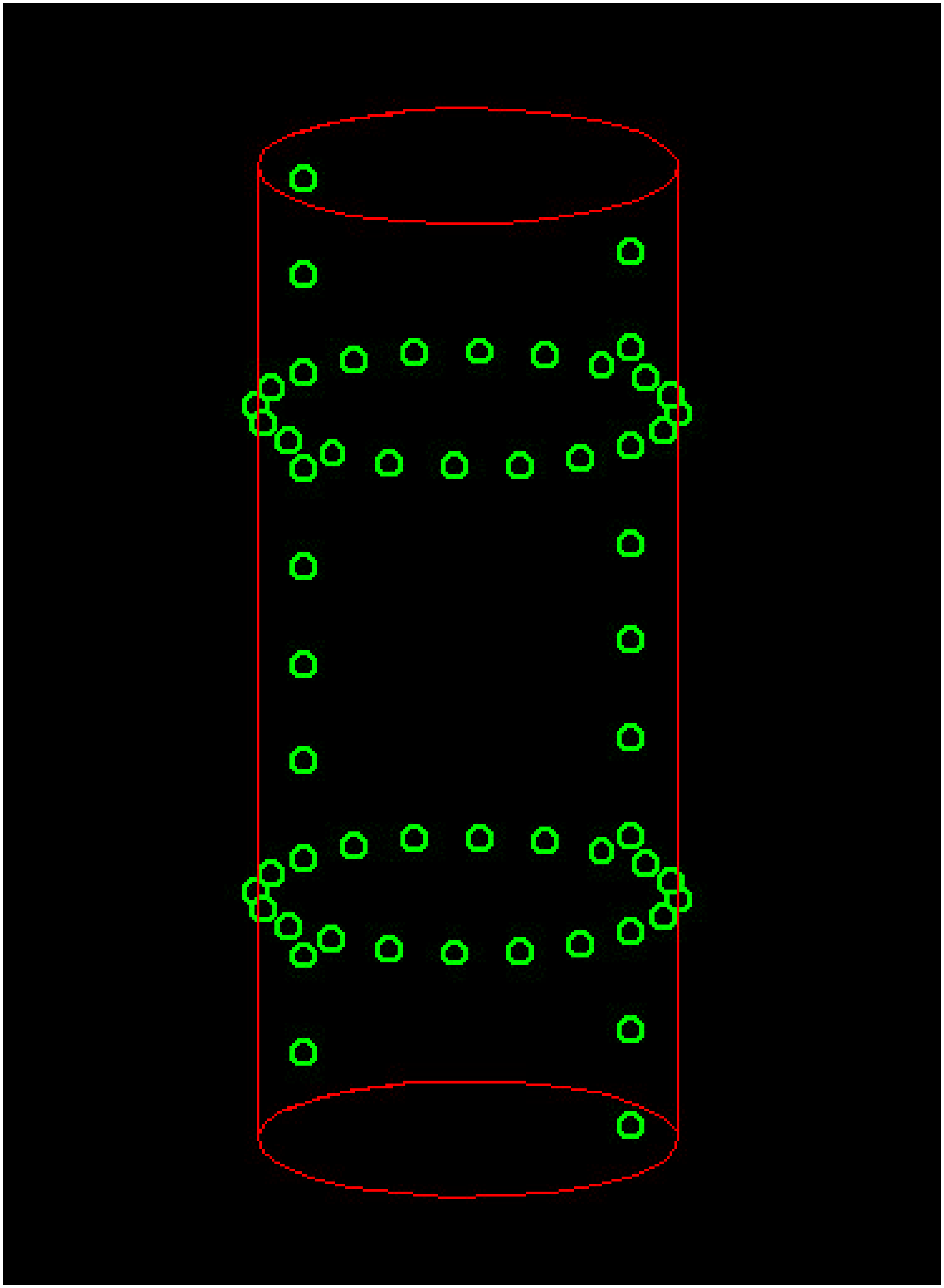

Figure 3. A 3-dimensional view of the acoustic tomographic pulse transmission array.

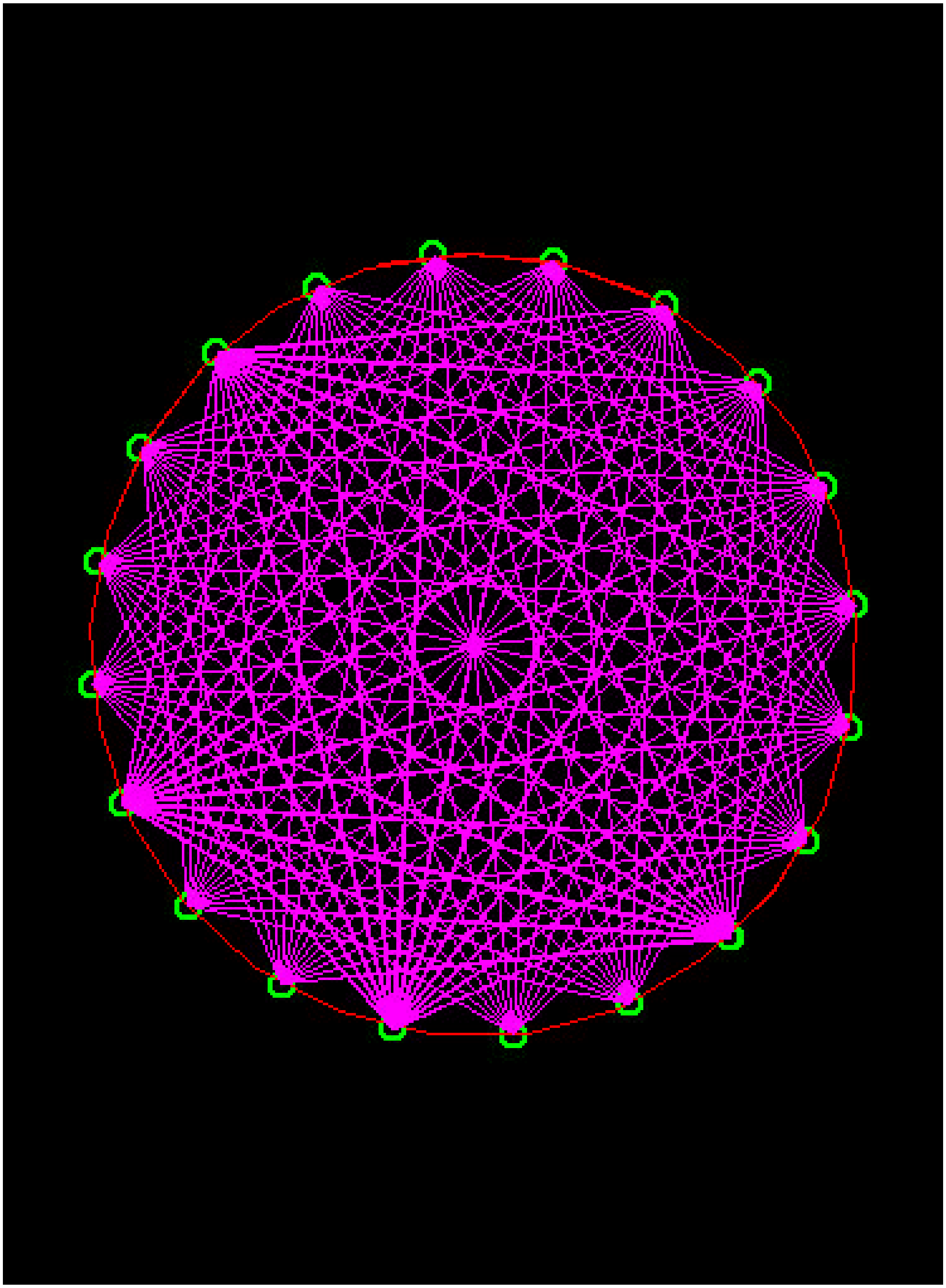

Figure 4. A top view of the acoustic raypaths in a horizontal plane.

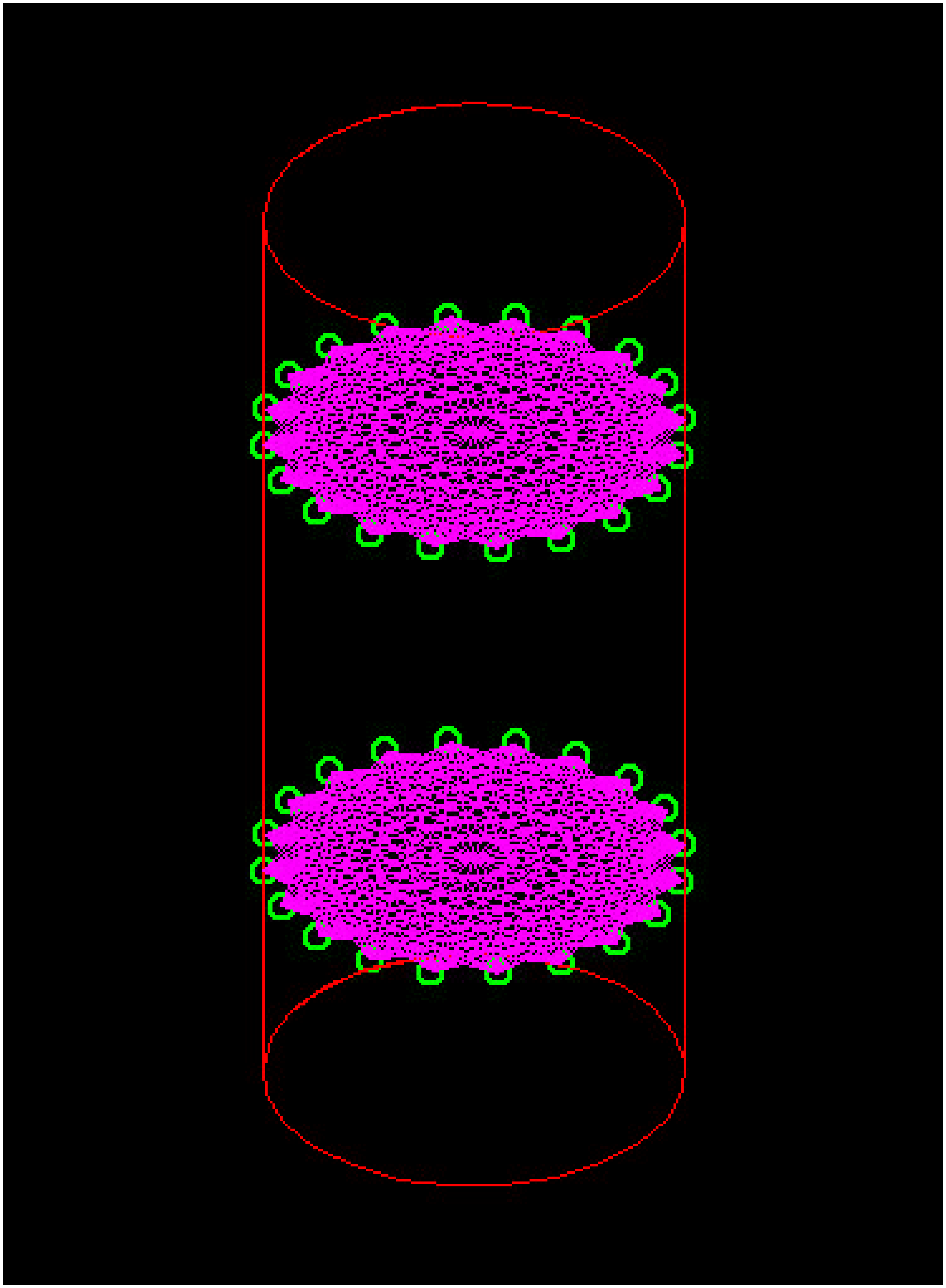

Figure 5. 3-dimensional locations of the horizontal tomographic imaging planes.

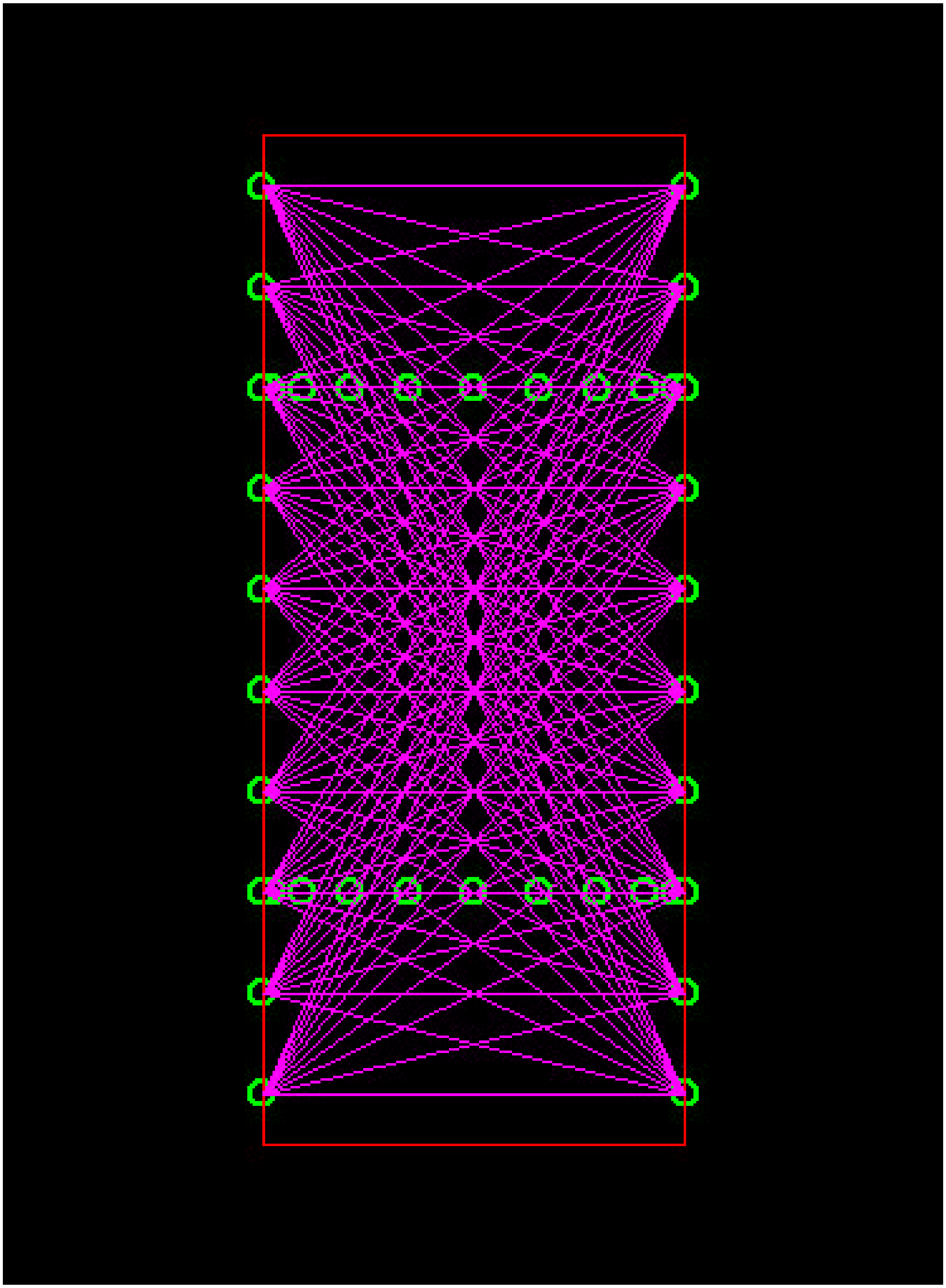

Figure 6. A side view of the acoustic raypaths in the X-Z plane.

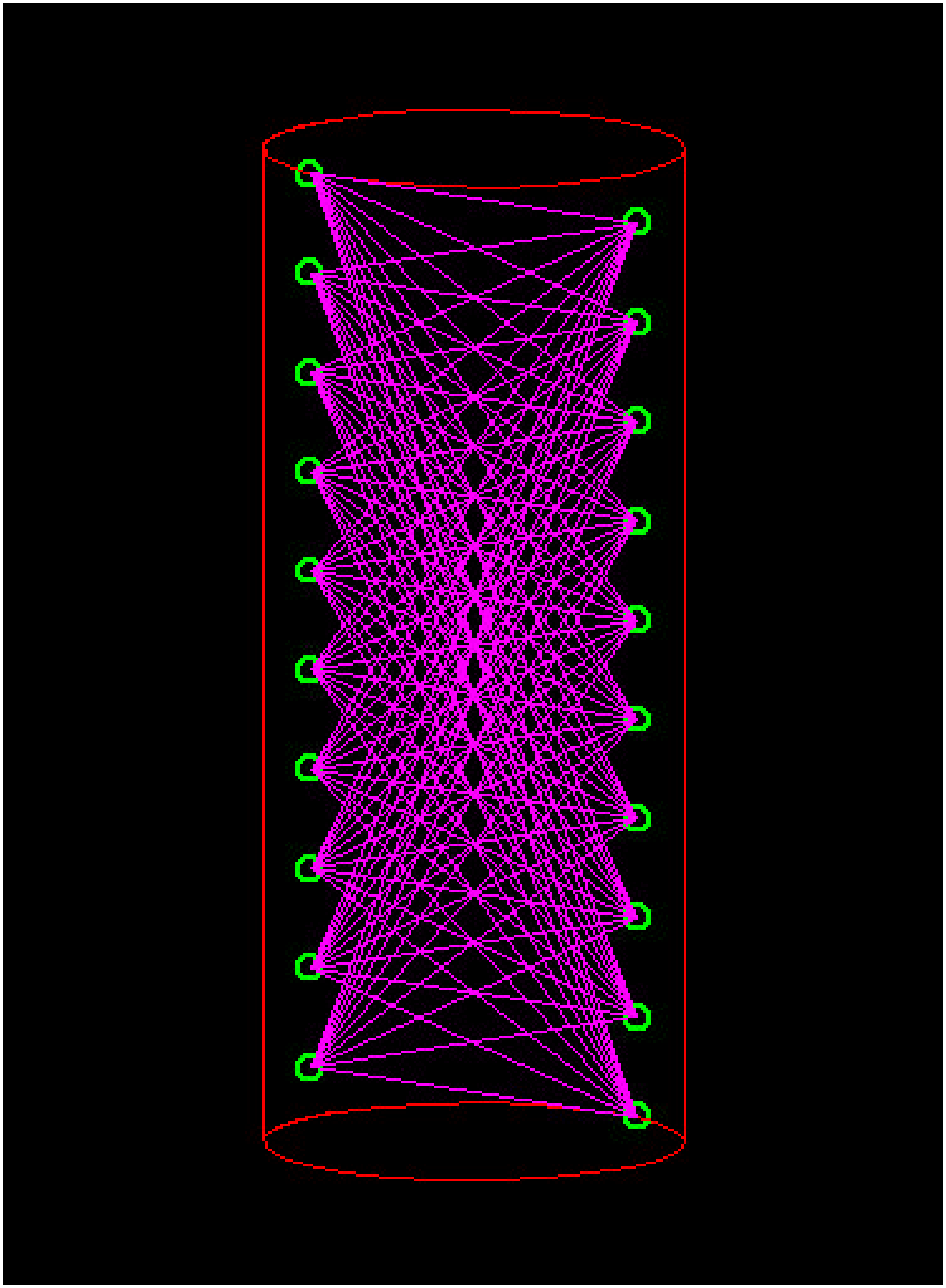

Figure 7. A 3-dimensional view of the acoustic raypaths in the vertical imaging plane.

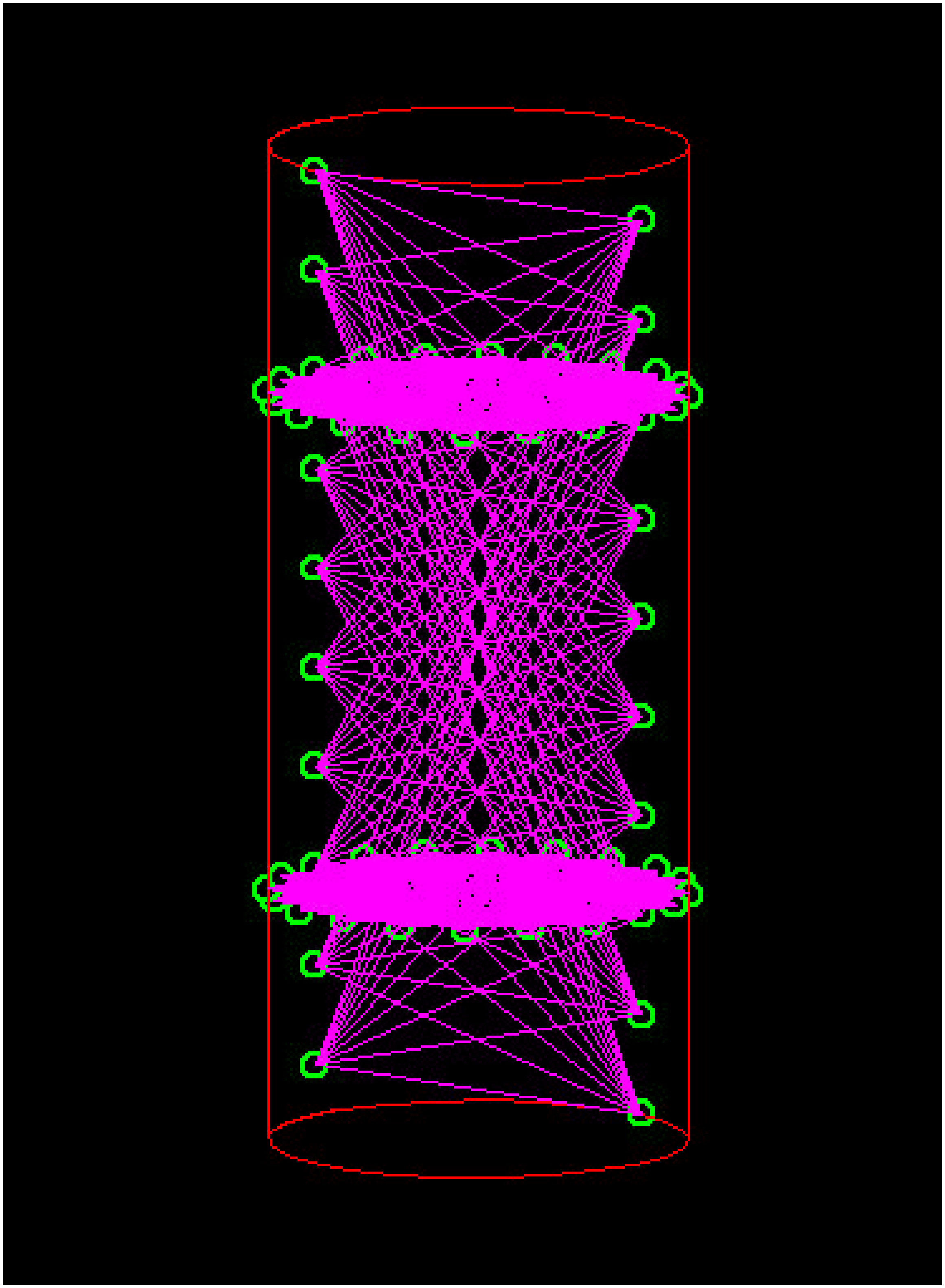

Figure 8. A 3-dimensional view of all the acoustic raypaths in the rock sample. There are a total of 620 acoustic raypaths in the projection.